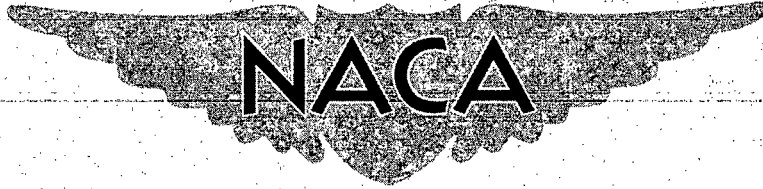


NACA RM L56E01



# RESEARCH MEMORANDUM

A SEMIEMPIRICAL PROCEDURE FOR ESTIMATING WING BUFFET

LOADS IN THE TRANSONIC REGION

By T. H. Skopinski and Wilber B. Huston

Langley Aeronautical Laboratory  
Langley Field, Va.

CLASSIFICATION CHANGED

To UNCLASSIFIED

*NACA Results*

By authority of *1RN-127* Date *effective Dec 16, 1958*  
*ANT 6-16-58*

CLASSIFIED DOCUMENT

This material contains information affecting the National Defense of the United States within the meaning of the espionage laws, Title 18, U.S.C., Secs. 793 and 794, the transmission or revelation of which in any manner to an unauthorized person is prohibited by law.

## NATIONAL ADVISORY COMMITTEE FOR AERONAUTICS

WASHINGTON

September 14, 1956

SEP 21 1956



## NATIONAL ADVISORY COMMITTEE FOR AERONAUTICS

## RESEARCH MEMORANDUM

A SEMIEMPIRICAL PROCEDURE FOR ESTIMATING WING BUFFET  
LOADS IN THE TRANSONIC REGION

By T. H. Skopinski and Wilber B. Huston

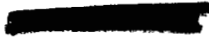
## SUMMARY

Wing buffeting data obtained from a flight loads investigation of two jet-propelled swept-wing airplanes were analyzed together with some published wind-tunnel results on two unswept-wing models to study the effects of Mach number and reduced frequency on the wing buffet loads. As a result of this analysis, a semiempirical procedure for estimating wing buffet loads in the transonic speed region was derived which appears to correlate the data from wings of different thickness ratios, stiffness, and size in the Mach number range from 0.65 to 1.0.

A study of a buffet-intensity-parameter variation with reduced frequency indicated consistent trends between the flight results and the wind-tunnel results. Including penetration and wing thickness ratio as parameters in an expression for the root-mean-square buffet moment at the wing root reveals Mach number effect as being a systematic departure from a faired curve which represented the wind-tunnel buffet-intensity-parameter variation with reduced frequency. This departure appeared to be fixed by the transition to critical flow and was a function of the product of the fundamental frequency and mean aerodynamic chord of the wing.

## INTRODUCTION

The concept of buffeting as the response of a simple elastic system to random forces associated with separated flow has been explored in a number of analytical and experimental studies (refs. 1 to 6). These analyses have indicated the validity of applying the methods of generalized harmonic analysis to the study of wing-buffet loads. For example, information presented in reference 5 has indicated a wind-tunnel technique for scaling the buffet loads obtained on simple wind-tunnel models to the loads expected for the airplane.



The purpose of the present investigation was to study the flight buffet-loads data obtained on two swept-wing jet-propelled airplanes and the wind-tunnel results presented in reference 5 and to examine the effects of Mach number and reduced frequency on the wing-buffet loads. As a result of this analysis a semiempirical procedure for a rough estimation of wing buffet loads which appears to correlate the data from wings of various thickness ratio, stiffness, and size has been derived.

## SYMBOLS

b	wing span, ft
c	wing chord, ft
$\bar{c}$	mean aerodynamic wing chord, ft
c(y)	wing chord distribution, ft
t/c	thickness ratio
y	spanwise coordinate from wing center line
y <sub>g</sub>	spanwise coordinate from wing center line to strain-gage location
q	dynamic pressure, lb/ft <sup>2</sup>
t	time, sec
Δt	increment in time, sec
C <sub>N</sub>	airplane normal-force coefficient
ΔC <sub>N</sub>	incremental normal-force coefficient or penetration above buffet boundary
C <sub>N</sub> $\left(\frac{\omega_1 c}{V}\right)$	buffet input spectrum at a given value of reduced frequency
C <sub>Lα</sub>	effective slope of lift curve for vibrating wing under conditions of separated flow
M	Mach number
V	airspeed, ft/sec

- BM incremental buffet moment, ft-lb
- $w_1(y)$  deflection of wing elastic axis in first wing bending, given in terms of a unit tip deflection
- $m(y)$  wing mass distribution, slugs/ft
- S wing area, ft<sup>2</sup>
- $S_1$  effective area in bending,  $2 \int_0^{b/2} c(y)w_1(y) dy$ , sq ft
- $S_2$  effective area in bending,  $2 \int_0^{b/2} c(y)w_1^2(y) dy$ , sq ft
- $M_W$  mass of wing,  $2 \int_0^{b/2} m(y) dy$ , slugs
- $M_1$  effective mass of wing in bending,  $2 \int_0^{b/2} m(y)w_1^2(y) dy$ , slugs
- $M_{m1}$  effective moment of mass outboard of point  $y_g$ ,  
 $\int_{y_g}^{b/2} (y - y_g)m(y)w_1(y) dy$ , slug-feet
- $F_S$  dimensionless structural factor,  $\frac{M_{m1}}{M_1} \frac{b}{2} \sqrt{\frac{\pi S_1^2 M_1}{8 S_2^2 S M_W}}$
- $k_S$  physical factor,  $\omega_1 \frac{b}{2} \sqrt{c S M_W}$ , ft<sup>2</sup>-lb<sup>1/2</sup>
- $\sigma_M$  root-mean-square value of incremental buffet bending moment, ft-lb
- $\omega_1$  circular frequency for first symmetrical wing bending, radians/sec

$\frac{\omega_1 \bar{c}}{V}$  reduced frequency

$\Phi \left( \frac{\omega_1 \bar{c}}{V} \right)$  buffet-intensity parameter per unit penetration,

$$\frac{\partial}{\partial \Delta C_N} \left[ \frac{C_N \left( \frac{\omega_1 \bar{c}}{V} \right)}{C_{L\alpha} \left( \frac{\omega_1 \bar{c}}{V} \right)} \right]^{1/2}$$

#### AIRPLANE AND INSTRUMENTATION

The flight test data of the present study were obtained on the North American F-86A fighter airplane and on the Douglas D-558-II research airplane. Flight tests on the F-86A airplane were conducted at the Ames Aeronautical Laboratory and those on the D-558-II airplane, at the NACA High-Speed Flight Station at Edwards, Calif. Both airplanes have swept wings and are jet-powered. Three-view drawings of the airplanes are shown in figure 1 and the airplane characteristics pertinent to the present study are summarized in table I.

Wing shear and bending-moment measurements were obtained from electrical wire resistance strain gages mounted on the spars near the wing root. For both test airplanes, standard strain-gage-calibration procedures (ref. 7) showed that the bridge mounted near the flange of the rear spar responded primarily to bending moment and was a reliable measure of the variation of the wing-root incremental bending moment.

The strain-gage responses were recorded on an 18-channel oscillograph which used galvanometer elements with a natural frequency of 100 cycles per second and which were damped to approximately 70 percent of critical. Standard NACA recording instruments synchronized by a common timer were used to measure all the pertinent quantities. The true Mach number for both airplanes was determined from a nose-boom airspeed system that measured both static and total pressure and was calibrated over the test Mach number range.

#### DATA AVAILABLE FOR ANALYSIS

Information on the correlation between buffeting intensity and penetration at various altitudes and airspeed was obtained from five selected flights that were a part of the two flight-research programs

conducted with the North American F-86A and the Douglas D-558-II airplanes. The flights analyzed were ones in which gradual pull-ups were made into the buffeting region. The Mach numbers for all the runs were held as constant as possible until a maximum acceleration was reached after which the Mach number was allowed to decrease gradually at these higher accelerations.

The gradual pull-up data analyzed for the F-86A airplane included nine runs of two flights at 35,000 feet at Mach numbers from about 0.60 to about 0.95 and six runs of a flight at an altitude of 45,000 feet covering a Mach number range from about 0.50 to about 0.90. The two flights of the D-558-II airplane which were analyzed included one run at 35,000 feet which covered a Mach number range from about 0.80 to about 0.95 and one run at an altitude of 25,000 feet which included buffeting data for Mach numbers between 0.65 and 0.80.

Selected for comparison are data obtained in the Langley 2- by 4-foot flutter research tunnel for two 4-percent-thick unswept semispan models with an aspect ratio of 4.0 and a taper ratio of 0.20. An angle of attack was selected that was considered to be representative of a penetration of approximately 0.30 in lift coefficient for a buffet boundary that was fairly flat. The tunnel tests were limited to Mach numbers below about 0.75.

In order to indicate the general character of the flight records, some representative time histories of Mach number, airplane normal-force coefficient, incremental buffeting moment, and the root-mean-square buffeting moment are shown in figure 2. The Mach number and normal-force coefficient were calculated every 0.10 second whereas the strain-gage records were read every 0.01 second in order to survey the loads from 0 to 50 cycle per second.

In order to obtain the root mean square of the incremental buffet moment, the component of the wing bending moment due to the airplane maneuver had to be removed. This was accomplished by filtering out the low-frequency component due to the maneuver with a numerical filter, the details of which are presented in reference 6. After a time history of the incremental buffet moment  $BM(t)$  was obtained, it was then possible to break this component into a series of overlapping 1/2-second intervals, to determine the root mean square for each interval by the formula

$$\sigma_M(t) = \left\{ \frac{1}{50} \sum_{t-.25}^{t+.24} [BM(t)]^2 \right\}^{1/2}$$

and to use it as a measure of intensity.

## RESULTS AND DISCUSSION

Analysis of the buffet data of the present investigation has been guided by the analytical expression

$$\sigma_M = \left( \omega_1 \frac{b}{2} \sqrt{\bar{c} S M_W} \right) \sqrt{q} F_S \left[ \frac{C_N \left( \frac{\omega_1 \bar{c}}{V} \right)}{C_{L_\alpha} \left( \frac{\omega_1 \bar{c}}{V} \right)} \right]^{1/2} \quad (1)$$

presented in reference 5 for the root-mean-square buffet moment at the wing root. The first term in the brackets includes the principal physical characteristics of the wing. The operating conditions are represented by the square root of the dynamic pressure. The quantity  $F_S$  is a dimensionless structural factor which reduces the actual values of wing area, mass, and moment arm to their effective values in the vibrating system. (See section on "Symbols" for expression defining these effective quantities.) The second bracketed term in equation (1) represents the ratio of a buffet input spectrum to the coefficient of aerodynamic damping. This ratio is for a particular value of reduced frequency corresponding to the fundamental bending frequency, the average chord, and the flight speed. Thus, equation (1) indicates that speed changes would affect buffet loads in two ways. A direct effect is through variations in dynamic pressure, the loads being directly proportional to the square root of the dynamic pressure and thus to the first power of the speed for a system with aerodynamic damping. The loads would also be affected through changes in the ratio of the input forces and the damping which were functions of reduced frequency.

In addition to the two speed effects noted in equation (1), buffet loads at transonic speeds have been found in references 4, 5, and 6 to vary linearly with penetration above the buffet boundary so that the expression for the root-mean-square buffet moment at the wing root for transonic speed can be taken as

$$\sigma_M = \left( \omega_1 \frac{b}{2} \sqrt{\bar{c} S M_W} \right) \sqrt{q} F_S \frac{\partial}{\partial \Delta C_N} \left[ \frac{C_N \left( \frac{\omega_1 \bar{c}}{V} \right)}{C_{L_\alpha} \left( \frac{\omega_1 \bar{c}}{V} \right)} \right]^{1/2} \Delta C_N \quad (2)$$

or for simplicity

$$\sigma_M = k_S \sqrt{q} F_S \phi \left( \frac{\omega_1 \bar{c}}{V} \right) \Delta C_N \quad (3)$$

where the principal physical characteristics of the wing are represented by the factor

$$k_S = \omega_1 \frac{b}{2} \sqrt{\bar{c} S M_W}$$

and where the aerodynamic forces are represented by a buffet-intensity parameter

$$\phi \left( \frac{\omega_1 \bar{c}}{V} \right) = \frac{\partial}{\partial \Delta C_N} \left[ \frac{C_N \left( \frac{\omega_1 \bar{c}}{V} \right)}{C_{L\alpha} \left( \frac{\omega_1 \bar{c}}{V} \right)} \right]^{1/2}$$

Wind-tunnel tests which were run on a family of related 4-percent-thick unswept wings have shown a variation of the buffeting parameter

$$\left[ \frac{C_N \left( \frac{\omega_1 \bar{c}}{V} \right)}{C_{L\alpha} \left( \frac{\omega_1 \bar{c}}{V} \right)} \right]^{1/2}$$

with reduced frequency and have also indicated (ref. 5) an effect of Mach number at the lower values of reduced frequency corresponding to Mach numbers greater than about 0.65. In the present analysis of the available buffet data on two swept wings, an attempt has been made to separate the effects of penetration and dynamic pressure in order to examine the effects of Mach number and reduced frequency on the buffet-intensity parameter.

#### Variation With Penetration and Dynamic Pressure

In order to analyze the variation of buffet intensity with penetration for the Mach number range covered by the tests, the buffet boundaries

of the test airplanes were determined. The buffet boundaries for both airplanes are shown in figure 3. From a time history of  $M$  and  $C_N$ , the value of penetration  $\Delta C_N$  above the buffet boundary was obtained for the same time that  $\sigma_M(t)$  was calculated. The resulting plot of  $\sigma_M/\sqrt{q}$  as a function of penetration for different Mach numbers is shown in figure 4. Variation of buffet intensity with altitude appears to be accounted for when  $\sigma_M$  is divided by  $\sqrt{q}$  in agreement with analytical results for the case where aerodynamic damping predominates. The results for both airplanes indicate a reasonably linear variation of buffet intensity with penetration beyond the buffet boundary for the transonic speed range covered, and straight lines have been faired from the origin through the data for each Mach number.

#### Variation With Mach Number and Reduced Frequency

In order to study the effects of Mach number and reduced frequency on the buffet intensity parameter  $\phi\left(\frac{\omega_1 \bar{c}}{V}\right)$ , values of the slope corresponding to the straight-line fairings of figure 4 have been used together with values of  $k_S$  and  $F_S$  for the two wings. The parameters used to calculate the constant  $k_S$  and the dimensionless structural factor  $F_S$ , are given in table I for each of the two wings. The assumed shape of the deflection of the wing elastic axis in first wing bending used to calculate the effective areas, masses, and moments in the present study is given by the expression

$$w_1(y) = 1 - \cos \pi y/b \quad -\frac{b}{2} \leq y \leq \frac{b}{2}$$

where the deflection is given in terms of a unit tip deflection. Calculations made by using slightly different first bending mode shapes (obtained from refs. 8 and 9) indicate no appreciable effect of mode shape on the structural factor  $F_S$ .

The buffeting-intensity parameter calculated by the following expression:

$$\phi\left(\frac{\omega_1 \bar{c}}{V}\right) = \frac{\sigma_M}{\frac{1}{2} \Delta C_N k_S F_S q} \quad (4)$$

for the two test airplanes is shown in figure 5 for different values of reduced frequency  $\omega_1 \bar{c}/V$ . Also shown for comparison in figure 5 are the wind-tunnel results given in reference 5 for two unswept 4-percent-thick wing models. The mean line faired through the model data appears to represent a characteristic variation of the buffet-intensity parameter with reduced frequency. Dotted lines faired through both the flight and wind-tunnel data appear to represent a characteristic Mach number effect, a reduction of intensity with increasing speed. This variation attributed to Mach number effect can be thought of as being associated with a change in the area exposed to the fluctuating pressures in separated flow, thus, as the shock wave moves toward the wing trailing edge with increasing Mach number, the exposed area, and likewise the input, become smaller. The extrapolation shown in figure 5 to an intercept at a reduced frequency corresponding to sonic velocity was made on this basis.

Examination of the data in figure 5 shows much higher values of the intensity parameter for the thicker wings, a result which is not in conflict with the results of two-dimensional airfoil studies such as reference 10. This observation led to the empirical attempt to include the effects of airfoil thickness on buffeting intensity by simply dividing the intensity-parameter values presented in figure 5 by the thickness ratio or

$$\sigma_M = k_S \sqrt{q} F_S \frac{\Phi\left(\frac{\omega_1 \bar{c}}{V}\right)}{(t/c)} \Delta C_N \left(\frac{t}{c}\right) \quad (5)$$

The resulting thickness-modified buffeting-intensity-parameter values are shown in figure 6. Since the choice for the two swept wings was arbitrary, the root-thickness ratio perpendicular to the sweep axis was selected. The results in figure 6 indicate both agreement with and systematic departure from the solid line representing the intensity variation with reduced frequency. The reduced frequency at which this departure occurs is the value corresponding to a Mach number of approximately 0.65 indicated by the solid symbols. The departure from this line or shape is perhaps fixed by the transition to critical flow and is thus a function of the product  $\omega_1 \bar{c}$ .

In view of the marked differences in plan form and thickness ratio of the wings and the models of the present study, the consistency of the two sets of data shown in figure 6 is surprising and perhaps fortuitous. In particular, the indicated unimportance under separated flow conditions of sweep, taper, and aspect ratio as compared with thickness is in marked contrast to the state of affairs for potential flow and verification by a suitable series of systematic tests including higher values of sweep angle would be desirable. Yet the consistency shown in figure 6 is such

as to encourage a hope that these data together with equation (5) would permit a rough estimate in the design stages of the buffet loads for a given wing in the Mach number range 0.65 to 1.0. For such application, it is believed that the linear dependence on thickness ratio should not be expected to hold for thickness ratios less than 4 percent.

### Estimation of Wing Buffet Loads

In order to illustrate the empirical procedure outlined in this paper the variation of buffet load with Mach number has been estimated for the 4-percent- and the 10-percent-thick wings of the X-1 series airplanes. The areas of these two wings are the same but, in addition to the difference in wing thickness ratio, the wing natural frequency, mean aerodynamic chord, aspect ratio, and mass differ; thus, a change of all the parameters in equation (5) is involved. Since a limited amount of experimental wing-buffet-load data (ref. 11) were available for the 10-percent thick wing at an altitude of approximately 20,000 feet, estimates of the variation per unit thickness of the buffet intensity parameter with reduced frequency were made for this altitude. Figure 7 is presented to show the estimated reduced-frequency variation of the intensity parameter which departs from the basic curve at a value of reduced frequency corresponding to a Mach number of 0.65 and then decreases rapidly to zero at a reduced frequency corresponding to sonic velocity. After

the estimated values of  $\frac{\Phi\left(\frac{\omega_1 \bar{c}}{V}\right)}{(t/c)}$  together with the necessary parameters

in equation (5) were known, it was possible to calculate the variation of root-mean-square buffet moment per unit penetration with Mach number. The calculated values of  $\sigma_M/\Delta C_N$  shown in figure 8 for the two wings indicate a much smaller wing root buffet moment for the thinner wing at a given penetration into the buffet region. On the basis of the effective areas, masses, and moments calculated for the two wings, the physical factor  $k_S$  influences the magnitude of the buffet load more than does the structural factor  $F_S$ .

In order to obtain some indication of the accuracy of the estimated buffet loads for the 10-percent-thick X-1 wing the published flight results of the X-1 airplane were analyzed. The wing-root buffeting shear loads presented in reference 11 are one-half the maximum peak-to-peak shear fluctuations in time intervals of approximately 1/2 second. From reference 4 the root mean square for a 1/2-second sample and a wing natural frequency of 14 cycles per second is estimated to be approximately one-half the maximum value. An assumption that the wing lateral centers of lift presented in reference 11 were approximately equal to the centers of the buffeting load was made to obtain a value of the root-mean-square buffet moment. The data for Mach numbers of approximately 0.76 and 0.79

at an airplane lift coefficient of approximately 0.82 give the values of  $\sigma_M/\Delta C_N$  shown as symbols in figure 8. The flight-test results agree reasonably well with the semiempirical procedure for obtaining an estimate of the wing buffet moment.

#### CONCLUDING REMARKS

The semiempirical procedure for estimating wing buffet loads suggested by the present analysis appears to correlate the data from wings of various thickness ratio, stiffness, and size. It is intended to provide a simple engineering method of obtaining a rough estimate in the design stages of the buffet loads for a given wing in the Mach number range from 0.65 to 1.0.

The following remarks may be made with regards to the analysis of the available wing buffet data to study the effects of Mach number and reduced frequency on the wing buffet loads. Including penetration and wing thickness ratio as parameters in an expression for the root-mean-square buffet moment at the wing root revealed Mach number effect as being a systematic departure from a faired curve which appeared to represent a characteristic variation of the buffet intensity parameter with reduced frequency. The departure from the curve representing reduced-frequency effect was perhaps fixed by the transition to critical flow and was a function of the product of the first bending frequency and average chord  $\omega_1 \bar{c}$ . In view of the marked differences in plan form and thickness ratio of the wings and the models of the present study, the consistency of the two sets of data was surprising and perhaps fortuitous. Verification by a suitable series of systematic tests including higher values of sweep angle would be desirable.

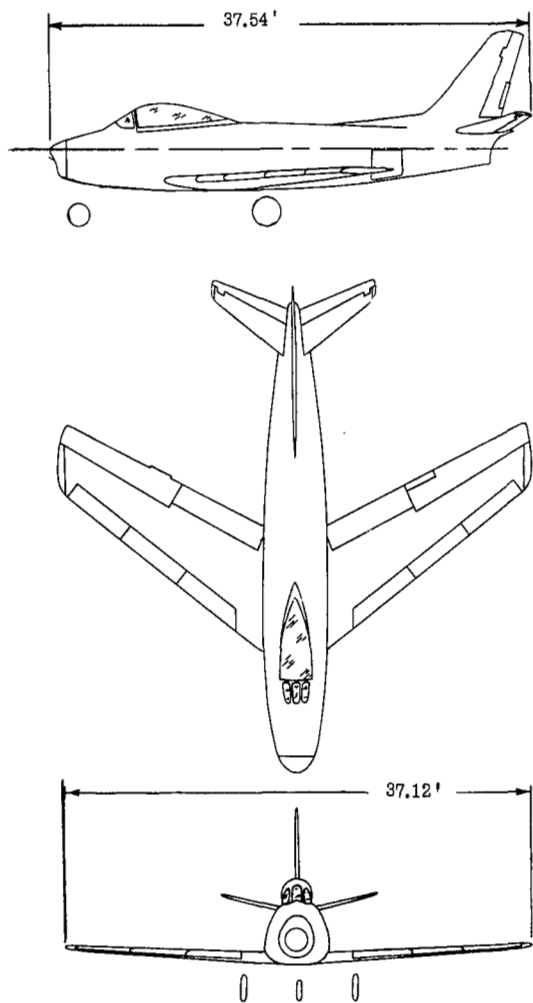
Langley Aeronautical Laboratory,  
National Advisory Committee for Aeronautics,  
Langley Field, Va., April 19, 1956.

## REFERENCES

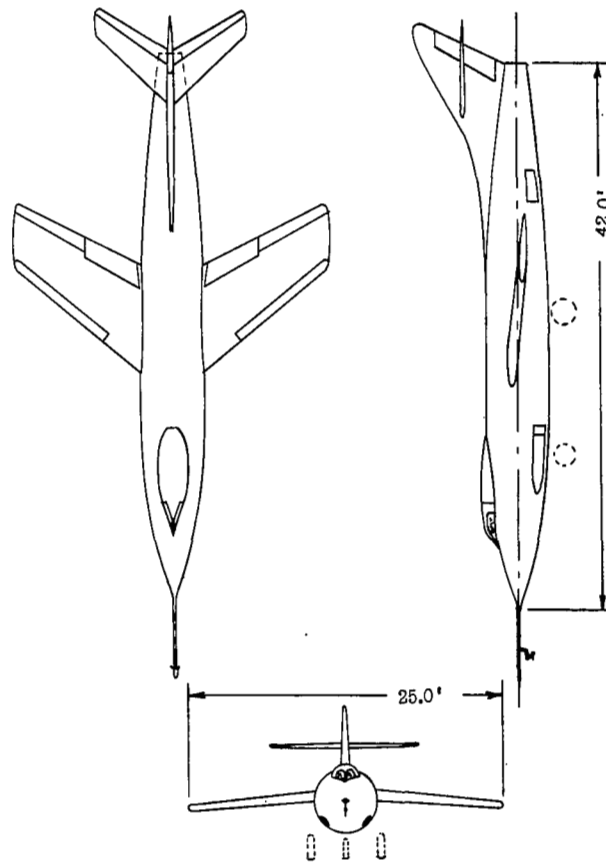
1. Liepmann, H. W.: On the Application of Statistical Concepts to the Buffeting Problem. Jour. Aero. Sci., vol. 19, no. 12, Dec. 1952, pp. 793-800, 822.
2. Liepmann, H. W.: Parameters for Use in Buffeting Flight Tests. Rep. No. SM-14631, Douglas Aircraft Co., Inc., Jan. 3, 1953.
3. Miles, John W.: An Approach to the Buffeting of Aircraft Structures by Jets. Rep. No. SM-14795, Douglas Aircraft Co., Inc. June 1953.
4. Huston, Wilber B., and Skopinski, T. H.: Measurement and Analysis of Wing and Tail Buffeting Loads on a Fighter Airplane. NACA Rep. 1219, 1955. (Supersedes NACA TN 3080.)
5. Huston, Wilber B., Rainey, A. Gerald, and Baker, Thomas F.: A Study of the Correlation Between Flight and Wind-Tunnel Buffeting Loads. NACA RM L55E16b, 1955.
6. Huston, Wilber B., and Skopinski, T. H.: Probability and Frequency Characteristics of Some Flight Buffet Loads. NACA TN 3733, 1956.
7. Skopinski, T. H., Aiken, William S., Jr., and Huston, Wilber B.: Calibration of Strain-Gage Installations in Aircraft Structures for the Measurement of Flight Loads. NACA Rep. 1178, 1954. (Supersedes NACA TN 2993.)
8. Young, Dana, and Felgar, Robert P., Jr.: Tables of Characteristic Functions Representing Normal Modes of Vibration of a Beam. Univ. of Texas Pub. No. 4913, Eng. Res. Ser. No. 44, Bur. Eng. Res., July 1, 1949.
9. Houbolt, John C., and Anderson, Roger A.: Calculation of Uncoupled Modes and Frequencies in Bending or Torsion of Nonuniform Beams. NACA TN 1522, 1948.
10. Polentz, Perry P., Page, William A., and Levy, Leonard L., Jr.: The Unsteady Normal-Force Characteristics of Selected NACA Profiles at High Subsonic Mach Numbers. NACA RM A55C02, 1955.
11. Beeler, De E., and Mayer, John P.: Measurements of the Wing and Tail Loads During the Acceptance Tests of Bell XS-1 Research Airplane. NACA RM L7L12, 1948.

TABLE I.- PHYSICAL CHARACTERISTICS OF TEST AIRPLANES

Item	Airplane	
	North American F-86A	Douglas D-558-II
Root airfoil section . . . . .	NACA 0012-64 (normal to 0.25-chord line)	NACA 63-010 (normal to 0.30-chord line)
Tip airfoil section . . . . .	NACA 0011-64 (normal to 0.25-chord line)	NACA 63-012 (normal to 0.30-chord line)
Dihedral angle, deg . . . . .	3.00	-3.00
Geometric twist, deg . . . . .	2.00	0
Sweep, deg . . . . .	34.23 (0.25-chord line)	35.00 (0.30 chord line)
Taper ratio . . . . .	0.51	0.56
Aspect ratio . . . . .	4.79	3.57
Span b, ft . . . . .	37.12	25.00
Mean aerodynamic chord, $\bar{c}$ ft . . . . .	8.08	7.27
Total area, S, sq ft . . . . .	287.90	175.00
Primary bending frequency $S_1$ , cps . . . . .	8.00	12.50
Effective area in bending, $S_1$ , sq ft . . . . .	88.20	55.00
Effective area in bending, $S_2$ , sq ft . . . . .	51.80	33.00
Wing mass, $M_W$ , slugs . . . . .	48.14	35.40
Effective mass, $M_1$ , slugs . . . . .	8.23	6.52
Effective moment of mass, $M_m$ , slug-ft . . . . .	146.27	69.10
Dimensionless structural factor, $F_S$ . . . . .	0.18	0.17
Physical factor, $k_S$ , $ft^2-lb^{1/2}$ . . . . .	$31.3 \times 10^4$	$20.8 \times 10^4$



(a) North American F-86A.



(b) Douglas D-558-II

Figure 1.- Three-view drawings of test airplanes.

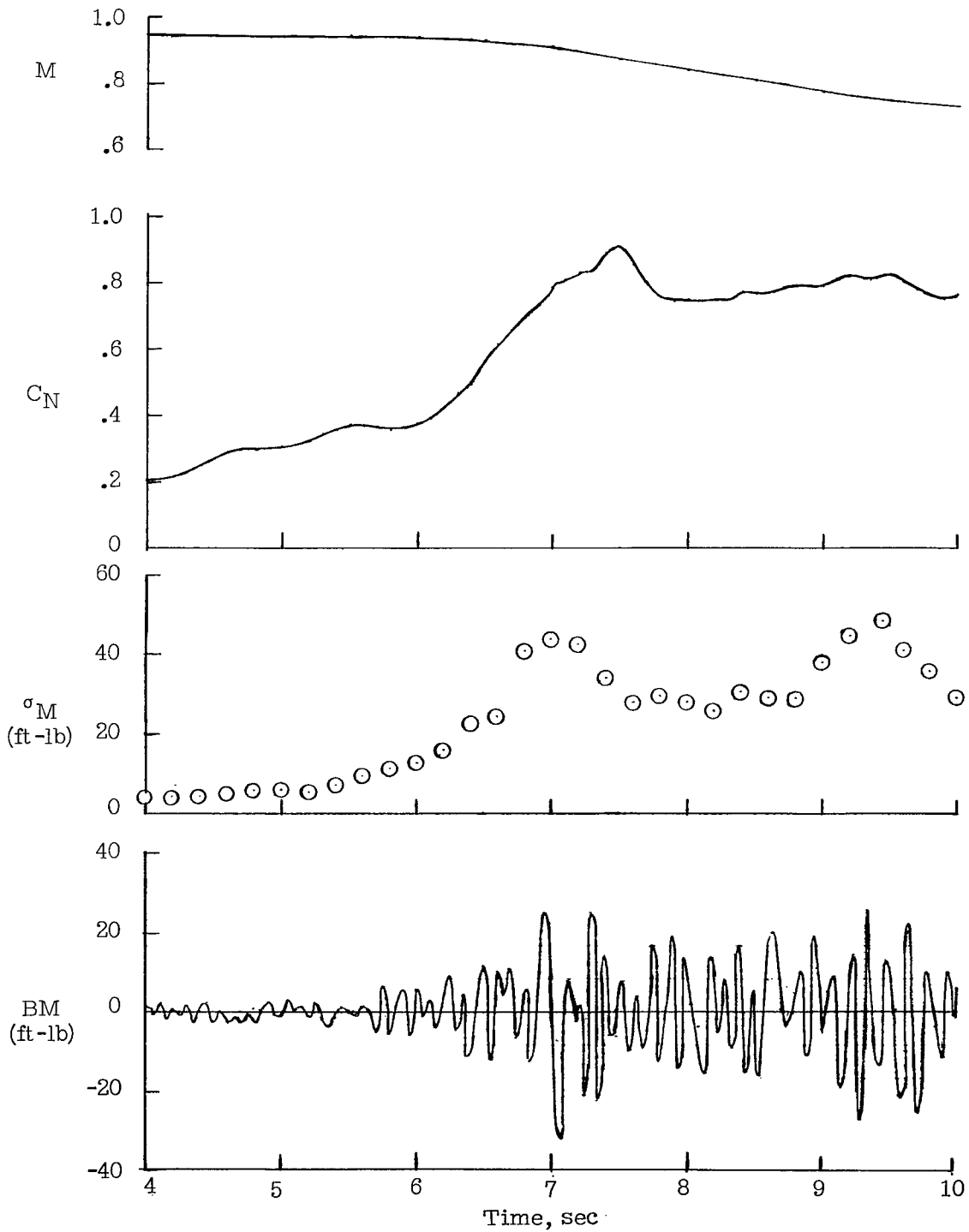
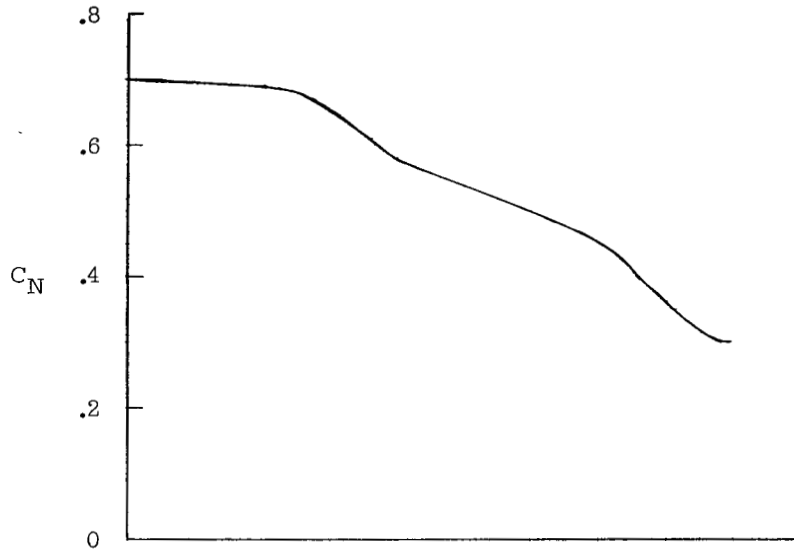
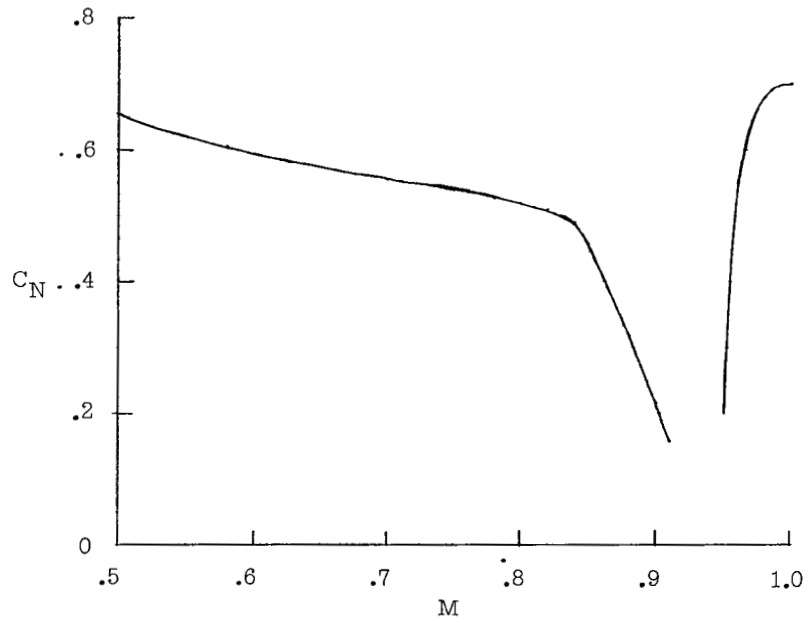


Figure 2.- Typical time history of parameters used in present analysis of wing buffeting.

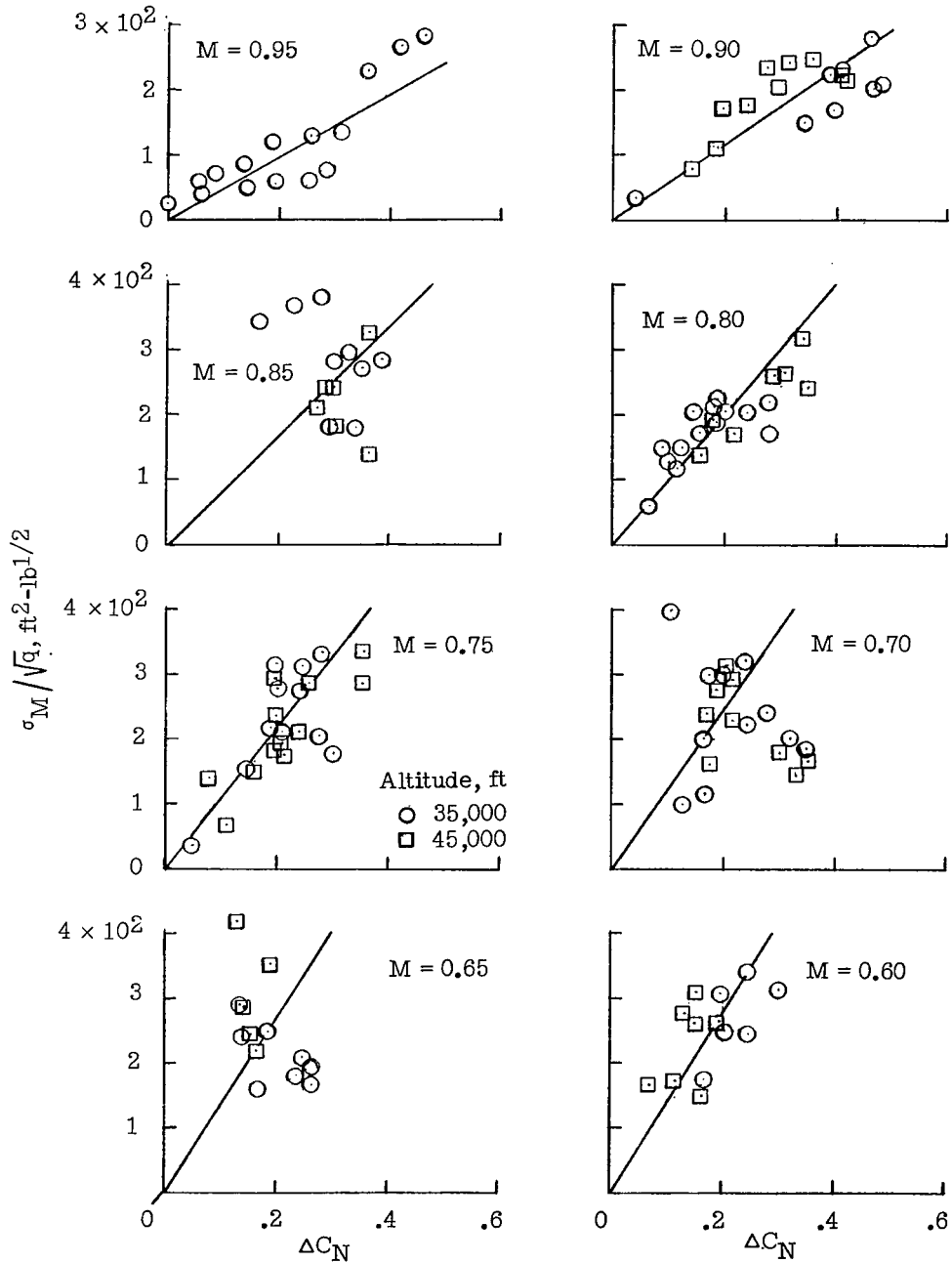


(a) North American F-86A airplane.



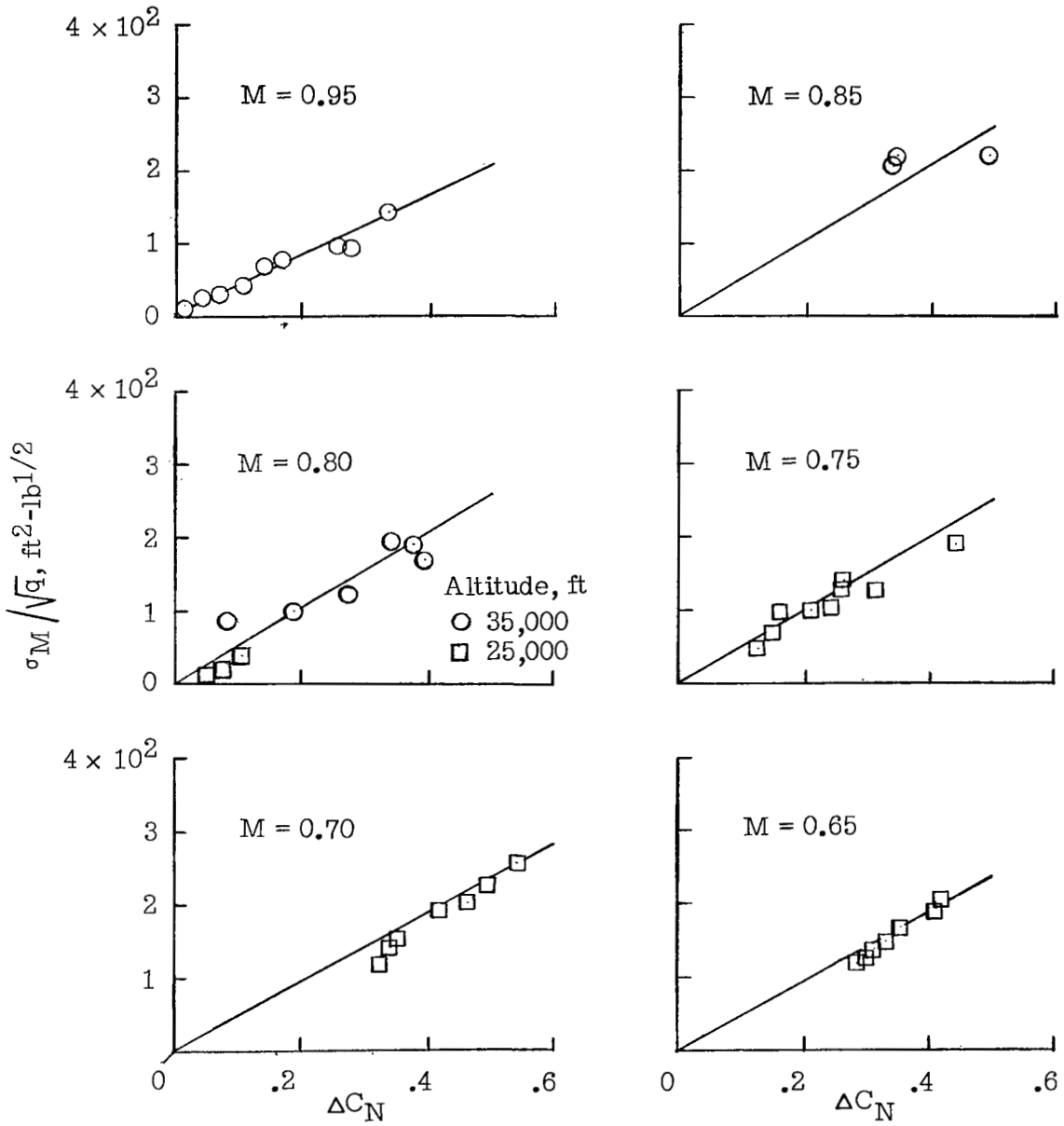
(b) Douglas D-558-II airplane.

Figure 3.- Buffet boundaries of test airplanes.



(a) North American F-86A airplane.

Figure 4.- Variation of  $\sigma_M / q^{1/2}$  with penetration at different Mach numbers for the two test airplanes.



(b) Douglas D-558-II airplane.

Figure 4.- Concluded.

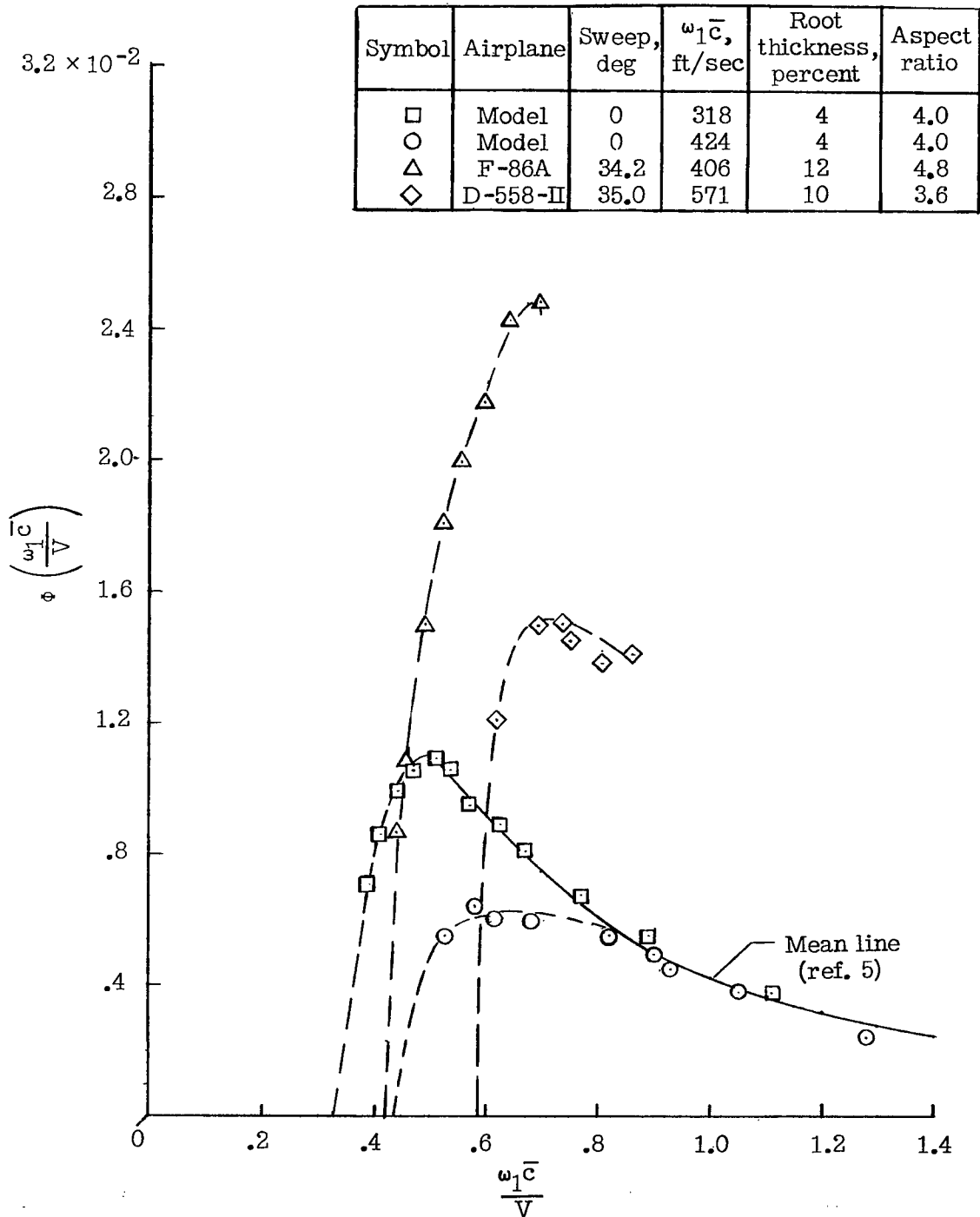


Figure 5.- Variation of buffeting-intensity parameter with reduced frequency for test airplanes and wind-tunnel wing models.

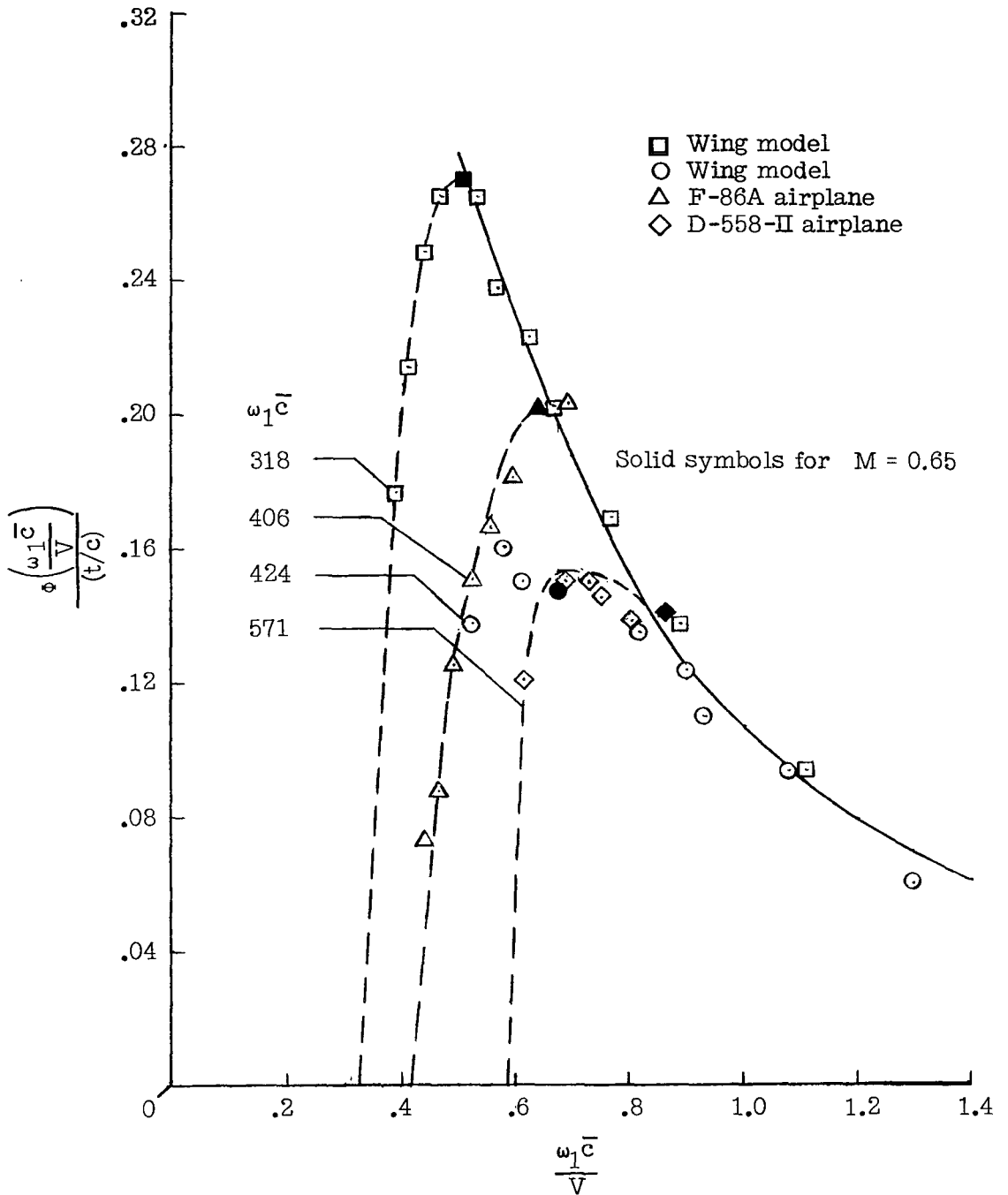


Figure 6.- Variation per unit thickness ratio of buffeting-intensity parameter with reduced frequency.

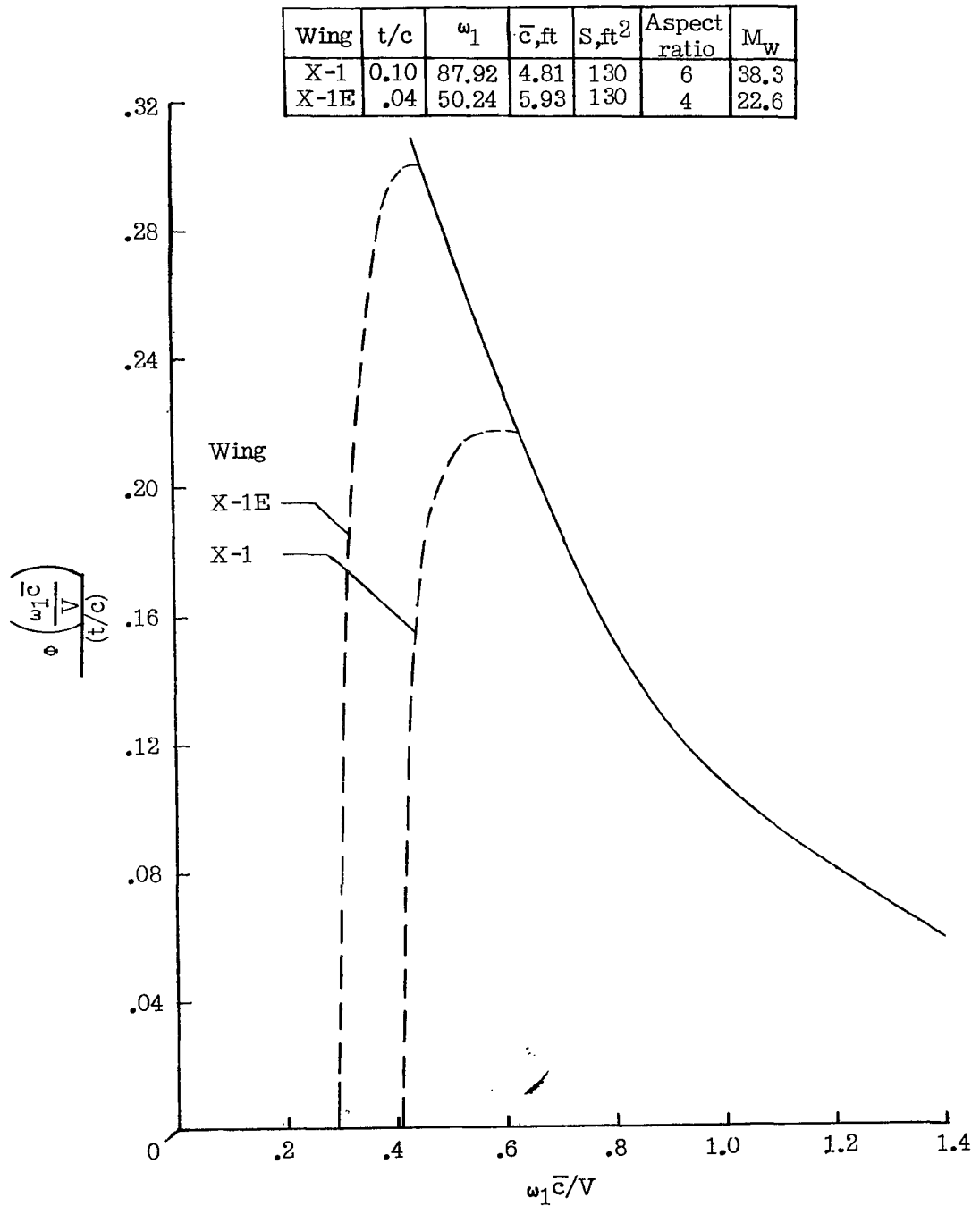


Figure 7.- Estimated variation with reduced frequency of a buffet-intensity parameter per unit thickness ratio for the wings of the Bell X-1 and X-1E airplanes.  $h_p = 20,000$  feet.

Wing	t/c	$\omega_1$	$\bar{c}$ ,ft	b,ft	S,ft <sup>2</sup>	F <sub>s</sub>	$\omega \frac{b}{2} \sqrt{\bar{c} S M_w}$
X-1	0.10	87.92	4.81	28.0	130	0.166	$14.64 \times 10^4$
X-1E	.04	50.24	5.93	22.8	130	.174	9.96

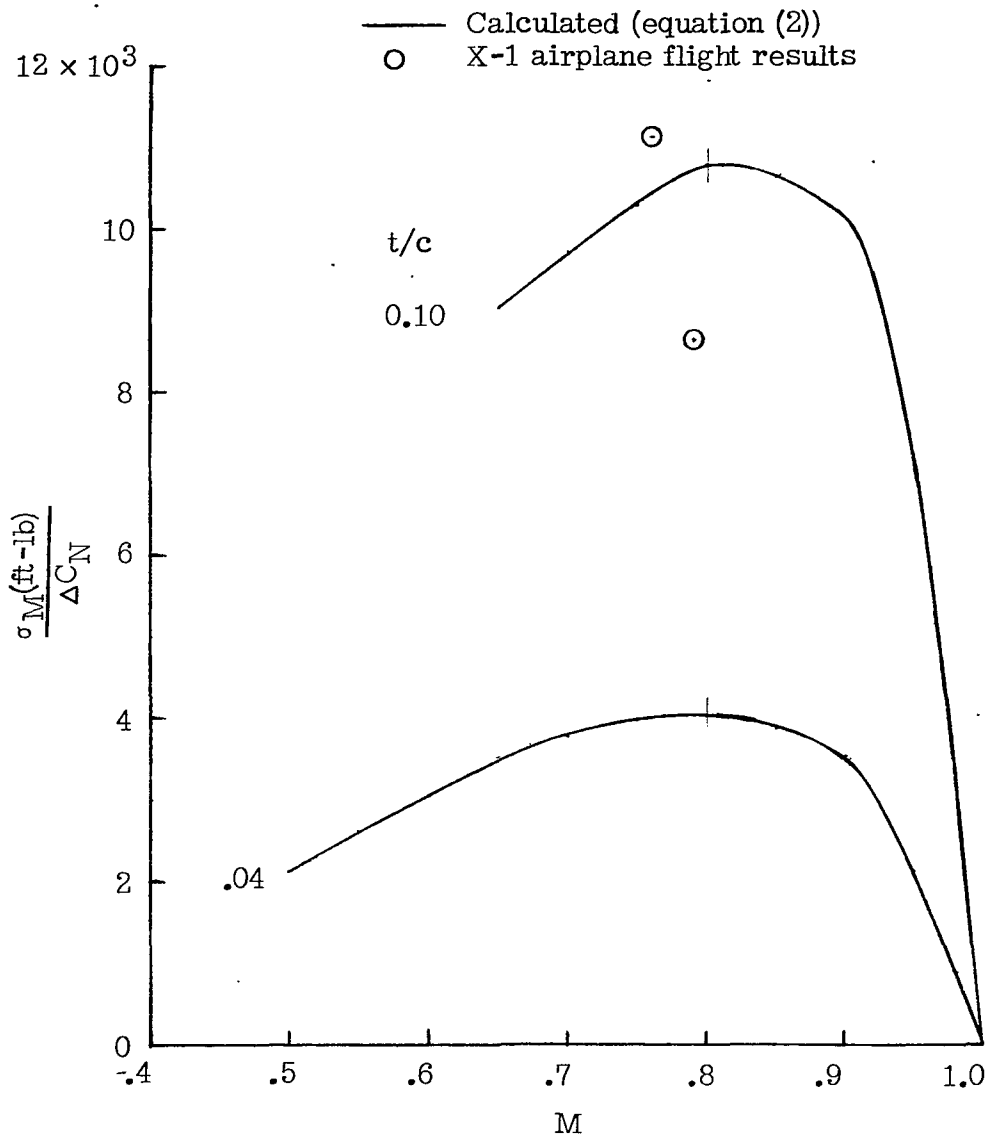


Figure 8.- Comparison between the estimated buffet moment per unit penetration of the 4- and the 10-percent-thick wings at various Mach numbers and two values obtained from the flight results with the 10-percent-thick wing.  $h_p = 20,000$  feet.

NASA Technical Library



3 1176 01437 2222

~~CONFIDENTIAL~~